

# Identifying the Potential Diagnostic Gene Biomarkers and Forecasting the Potential Therapeutic Agents for Advanced Diabetic Nephropathy Based on Pyroptosis and Ferroptosis

Qin Dai <sup>1,2</sup>, Siyi Huang <sup>3</sup>, Yi Fang<sup>4</sup>, Xiaoqiang Ding<sup>4</sup>

<sup>1</sup>Department of Nephrology, Xuhui District Central Hospital, Shanghai, People's Republic of China; <sup>2</sup>Department of Nephrology, Zhongshan-Xuhui Hospital, Fudan University, Shanghai, People's Republic of China; <sup>3</sup>Department of Nephrology, Ruijin Hospital, Shanghai Jiaotong University School of Medicine, Shanghai, People's Republic of China; <sup>4</sup>Department of Nephrology, Zhongshan Hospital, Fudan University, Shanghai, People's Republic of China

Correspondence: Yi Fang; Xiaoqiang Ding, Department of Nephrology, Zhongshan Hospital, Fudan University, Shanghai, 200032, People's Republic of China, Email fang\_yi2022@163.com; xq\_ding@126.com

**Background:** Diabetic nephropathy (DN) is a prevalent complication of diabetes, often leading to end-stage kidney disease (ESKD). Advanced DN progresses to ESKD rapidly, yet effective diagnostic indicators and treatments are lacking.

**Methods:** Two DN-related datasets were obtained from the Gene Expression Omnibus (GEO) database. Differentially expressed genes (DEGs) were identified using the R packages. Pyroptosis-related genes (PRGs) and ferroptosis-related genes (FRGs) were collected from their respective database. Pyroptosis- and ferroptosis-related differentially expressed genes (PFRDEGs) were identified by overlapping DEGs, PRGs, and FRGs for further analysis, including functional enrichment and immune infiltration. Hub genes were identified using a PPI network via MCODE-plugin in Cytoscape. GeneMANIA was utilized to explore intermolecular interactions among hub genes. Based on these hub genes, a diagnostic model was constructed using the receiver operating characteristic curve and potential therapeutic agents were retrieved. Correlation analysis between hub genes and estimated glomerular filtration rate was performed using Nephroseq v5 database, and expression of hub genes was validated in external GEO database, Nephroseq v5 database and DN mice in vivo.

**Results:** Four hub genes (CYBB, LCN2, JUN and ADIPOQ) were identified, and three of the four hub genes (CYBB, LCN2 and ADIPOQ) were found to be potential biomarkers for advanced DN. On this basis, three potential therapeutic agents were screened. More importantly, a series of biological experiments confirmed that CYBB and LCN2 were significantly up-regulated in DN mice.

**Conclusion:** This study identifies three hub genes as diagnostic biomarkers and mines three potential therapeutic agents for advanced DN, providing new insights into the role of pyroptosis and ferroptosis in advanced DN and laying the foundation for future research.

**Keywords:** diabetic nephropathy, pyroptosis, ferroptosis, bioinformatics, diagnostic biomarkers

## Introduction

As an urgent challenge for public health,<sup>1</sup> diabetic nephropathy (DN), also known as diabetic kidney disease, is a significant chronic microvascular complication of diabetes mellitus.<sup>2</sup> Globally, DN is the leading cause of CKD [including end-stage kidney disease (ESKD)] and an important risk factor for cardiovascular disease and early death in diabetic patients.<sup>3,4</sup> DN can be categorized into two groups as early DN and advanced DN according to the levels of urinary albumin-to-creatinine ratio (UACR) and renal function, and advanced DN was defined as UACR > 300mg/g or estimated glomerular filtration rate (eGFR) < 90mL/min.<sup>5</sup> Compared with early DN, patients with advanced DN have a higher risk of declining renal function and progression to ESKD.<sup>6</sup> Nevertheless, there is currently a lack of effective diagnostic means and treatments for advanced DN.

In terms of diagnostics, proteinuria and eGFR are nowadays crucial indicators for diagnosing DN, but they have their limitations. For example, among diabetic patients with massive proteinuria, approximately 70% of renal puncture biopsies confirm the presence of DN,<sup>7,8</sup> and only 40% of patients with type 2 diabetes and microalbuminuria exhibit the typical pathology of DN.<sup>9</sup> Furthermore, an increasing number of studies have discovered that diabetic patients with normal urinary albumin can still progress to DN, as evidenced by a decrease in eGFR to less than  $60\text{mL}\cdot\text{min}^{-1}$  ( $1.73\text{ m}^2$ )<sup>-1</sup> and the presence of typical DN in renal puncture pathology.<sup>8,10</sup> Above all, there is the absence of effective measures to diagnostic advanced DN. In terms of treatment, although new drugs such as SGLT-2i, DPP-4 inhibitors, and finerenone have provided additional treatment options for DN,<sup>11</sup> many patients with DN still progress to ESKD due to the limited effectiveness of the aforementioned drugs. Consequently, in-depth research on the pathogenesis of DN for identifying effective diagnostic biomarkers and exploring corresponding therapeutic agents will help to address these research gaps.

As a complex process involving multiple factors and mechanisms, the occurrence and development of DN is closely linked to the cell death.<sup>12</sup> Ferroptosis, one of the prominent research hotspots in cell death studies, was first proposed by Stockwell et al in 2012.<sup>13</sup> Nowadays increasing evidence suggests that ferroptosis is a key driver of DN.<sup>14–16</sup> Moreover, recent studies have demonstrated the efficacy of various small molecular agents, such as N-acetylcysteine, dapagliflozin, and salusin- $\beta$ , in improving renal function and alleviating kidney injury by suppressing ferroptosis.<sup>14</sup> On the other hand, pyroptosis is another recently identified mechanism of programmed cell death associated with caspase-1, which triggers a series of inflammatory responses through the release of multiple pro-inflammatory factors such as IL-1 $\beta$  and IL-18.<sup>17</sup> Recent studies also have reported that pyroptosis is related to the occurrence and development of DN, and that renal lesions in DN can be ameliorated by inhibiting the pyroptosis pathway.<sup>17–19</sup> As important indicators of pyroptosis, caspase-11 and gasdermin D (GSDMD) were found to be significantly overexpressed in mice with DN, accompanied by significantly elevated plasma levels of inflammatory factors such as NF- $\kappa$ B, IL-1 $\beta$ , and IL-18, which were downregulated by knockdown of *CASPASE-11* or *GSDMD*.<sup>20</sup> Furthermore, numerous findings have demonstrated that targeting the pertinent pathways of pyroptosis can effectively prevent the occurrence or delay the progression of DN. For instance, Pyrroloquinoline quinone ameliorates renal fibrosis in DN by inhibiting the pyroptosis pathway in C57BL/6 mice and human kidney-2 cells;<sup>18</sup> Inhibition of cellular death through targeted inhibition of caspase-1 significantly attenuates podocyte injury in DN mice;<sup>21</sup> and deletion of Gasdermin D significantly reduces the release of IL-1 $\beta$  and IL-18, thereby attenuating cellular pyroptosis and renal injury in diabetic mice in vivo.<sup>22</sup>

More importantly, A growing body of research suggests that multiple layers of interconnections exist between pyroptosis and ferroptosis, including shared triggers, molecular components and protective mechanisms.<sup>23–27</sup> More importantly, many recent studies have found that there is a mechanistic crosstalk between pyroptosis and ferroptosis, which provides new perspectives on the mechanistic study of the disease and new avenues for the treatment of the disease.<sup>28–31</sup> We therefore performed this study to explore potential diagnostic biomarkers linked to advanced DN from the viewpoints of both pyroptosis and ferroptosis by employing bioinformatics techniques. Besides, we also predicted the potential therapeutic agents targeting these biomarkers in an attempt to discover effective treatment measures for advanced DN. It is expected to provide new research perspectives for precise diagnosis and treatment for advanced DN.

## Material and Methods

### Data Source

For this study, we retrieved GSE142025 from the Gene Expression Omnibus (GEO) database that met the specified conditions using the keywords “diabetic nephropathy” or “diabetic kidney disease”. We then filtered out the dataset GSE30528 using the keywords “diabetic nephropathy” or “diabetic kidney disease” to meet the purpose of the study. The transcriptome datasets GSE142025 and GSE30528 were obtained from the National Center for Biotechnology Information (NCBI) / GEO database. GSE142025 was based on the Illumina HiSeq 4000 platform (Homo sapiens GPL20301).<sup>5,32</sup> Used as the primary objects of study, 21 advanced DN samples (GSM4217781–GSM4217801) and 9 control samples (GSM4217808–GSM4217816) were selected from the GSE142025 dataset, which was employed as the training dataset in the study ([Supplementary Table S1](#) presents the data of GSE142025 in detail). Additionally, Based on

the GPL571 platform of Affymetrix Human Genome U133A 2.0 Array,<sup>33,34</sup> GSE30528 includes 9 DN glomeruli samples (GSM756992–GSM757000) and 13 control glomeruli samples (GSM757001–GSM757013), and it was utilized as an external validation dataset ([Supplementary Table S2](#) presents the data of GSE30528 in detail). Clinical studies associated with GSE142025 was approved by the institutional review board at Shanghai Jiao Tong University Affiliated Sixth People's Hospital. Clinical studies associated with GSE30528 was approved by the institutional review board of the Albert Einstein College of Medicine and Montefiore Medical Center (2002–202 to K.S).

What's more, pyroptosis-related genes (PRGs) with protein encoding function were retrieved from the Genecards website (<https://www.proteinatlas.org/>, version 5.19) and the GSEA/Molecular Signatures Database (<https://www.gsea-msigdb.org/gsea/msigdb/>, version 4.3.3), and [Supplementary Table S3](#) presents the PRGs in detail. Ferroptosis-related genes (FRGs) were downloaded from FerrDb (<http://www.zhounan.org/ferrdb/current/>) and the GSEA/ Molecular Signatures Database (<https://www.gsea-msigdb.org/gsea/msigdb/>), [Supplementary Table S4](#) presents the FRGs in detail.

## Microarray Data Processing

The gene probe information was converted into gene symbols using the corresponding annotation profile in GSE30528. In cases where multiple probes corresponded to the same gene, the final gene expression value was determined by calculating the average expression value, and probes that did not map to genes were removed. The download and normalization of the raw matrix for GSE30528 was done with the “GEOquery” (version 2.72.0), “magrittr” (version 2.0.3), and “limma” (version 3.60.3) R packages. The raw matrix for GSE142025 were obtained by manual download and then collated. The standardized plots are provided as [Figure S1](#) in the supplementary materials.

## Screening the Differentially Expressed Genes (DEGs) and the Pyroptosis- and Ferroptosis-Related Differentially Expressed Genes (PFRDEGs)

The GSE142025 transcriptome dataset was analyzed using the “limma” R package (version 3.60.3). DEGs were identified based on adjusted  $P$  value  $< 0.05$  and  $|\log \text{fold change(FC)}| > 1$ . Heatmaps and volcano plots were used to visually represent the DEGs. The overlap among DEGs, PRGs and FRGs was visualized through a Venn diagram, displaying PFRDEGs.

## Gene Enrichment Analysis

Gene Ontology (GO) / Kyoto Encyclopedia of Genes and Genomes (KEGG) Pathway Enrichment Analysis for the PFRDEGs were performed by applying the “clusterProfiler” package for enrichment analysis in xiantao online website (<https://www.xiantaozi.com/>, version 2.0).<sup>35,36</sup> GO functional enrichment analysis include analysis of molecular function (MF), biological process (BP), and cellular component (CC) terms. In this study a gene set was regarded as significantly enriched if  $P_{\text{adj}} < 0.05$ . Gene Set Enrichment Analysis (GSEA) was performed to explore the potential biological processes of genes involved in advanced DN. GSEA was also performed by applying the “clusterProfiler” R package.  $P_{\text{adj}} < 0.05$  and FDR (q value)  $< 0.25$  was regarded as significantly enriched.

## Identifying Hub Genes and Exploring Intermolecular Interactions of PFRDEGs

To obtain hub genes for more in-depth analysis of the roles of pyroptosis and ferroptosis in advanced DN, STRING database (<https://string-db.org/>, version 11.5)<sup>37</sup> was utilized to create a protein–protein Interaction (PPI) network for PFRDEGs. MCODE-plugin of Cytoscape (version 3.9.0) was then employed to identify hub genes within the PPI network [Detailed parameters: Degree cutoff: 2; Cluster Finding: Haircut; Node Score Cutoff: 0.2; K-Core: 2; Max Depth: 100.]. GeneMANIA online software (<https://genemania.org/>) was utilized to delve intermolecular interactions among the four hub genes.

## Expression of Hub Genes in GSE142025 and Validation in External Dataset

Violin plots were used to visually detect differences in hub gene expression between the advanced DN cohort and the control group. In addition, to reduce the potential for false positives, hub gene expression was confirmed using an

independent DN dataset from the GEO database. For this validation, GSE30528 was selected, which contains data from 9 DN patients and 13 controls. Hub gene expression data was then acquired and presented using violin plots to facilitate comparative analysis.

## Analysis of Immune Infiltration and Correlations Between Hub Genes and Immune Cells

The CIBERSORTx algorithm serves as a sophisticated computational framework, adept at translating normalized gene expression data into detailed profiles of immune cell infiltration.<sup>38</sup> Leveraging the LM22 reference expression signature, we meticulously computed the relative frequencies of diverse immune cell types, differentiating between advanced DN patients and the control cohort, with the aid of the “CIBERSORT” R package (version 1.03). To deepen our understanding of the interplay between immune cells and pivotal hub genes, we conducted a thorough Pearson correlation analysis. The ensuing data were meticulously processed and rendered visually through the use of both boxplots and heatmaps, facilitated by an online platform (<https://www.xiantaozi.com/>, version 2.0).<sup>35,36</sup>

## Exploring the Correlation Between Hub Genes and Clinical Indicators

To explore the link between hub genes and clinical practice, we performed a data mining analysis between the expression of hub genes and eGFR utilizing the Nephroseq v5 database. The Nephroseq v5 database (<http://v5.nephroseq.org>, version 4)<sup>39</sup> is a robust information platform designed to evaluate the correlation between gene expression levels and clinical characteristics of kidney diseases. Additionally, we verified the hub genes expression in our study by cross-referencing it with data from this platform.

## Screening and Validation of Candidate Diagnostic Biomarkers

To further explore the clinical significance of the hub genes, receiver operating characteristic (ROC) curves were constructed to identify the potential diagnostic efficacy of the hub genes, which was evaluated based on the area under the curve (AUC). The ROC curves were generated using mRNA expression data from the GSE142025 dataset. The results were validated in the GSE30528 dataset. Statistical significance was set at  $P < 0.05$ .

## Identification of Potential Drug Candidates

To obtain potential agents for gene-targeted therapies for advanced DN, three small molecule compounds were retrieved from the ChEMBL database (<https://www.ebi.ac.uk/>, version 34) based on the hub genes. Information on the chemicals and their biological activities was obtained from the PubChem online website (<https://pubchem.ncbi.nlm.nih.gov>). The molecular formulae and two-dimensional structures of potential drugs were downloaded from the PubChem website to aid drug discovery.

## Validation of the Hub Genes in Animal Models for DN

### Animals and Reagents

C57BL/6 mice (SPF, male, 6–8 weeks old,  $20 \pm 2$ g) were purchased from the Finoco Biotechnology Co. (Shanghai, China). Mice were provided standard feed and water in a SPF grade animal facility. All animal experimental procedures were approved by the Animal Ethics committee of Finoco Biotechnology Co. (No. AUP-20240731-01) and were conducted in accordance with the National Institutes of Health Guide for the Care and Use of Laboratory Animals. Streptozocin (STZ) was purchased from Sigma Chemical Co. (Louis, USA). FastPure® Cell/Tissue Total RNA Isolation Kit V2, Reverse transcription kit HiScript III RT SuperMix for qPCR (+gDNA wiper, R323-01) and ChamQ Universal SYBR qPCR Master Mix (Q711-03) were purchased from Vazyme Biotech Co. (Nanjing, China).

### Animal Models

The mice were fed a high-fat diet for 4 weeks and then subjected to unilateral nephrectomy. One week after surgery, the mice were followed by intraperitoneal injection of STZ (50 mg/kg dissolved in 0.05 mol/L sterile sodium citrate, pH 4.5) for three consecutive days to induce diabetes. One week after the last STZ injection, animals with plasma glucose levels above 16.7 mmol/mL were considered successful model animals (ie C57BL/6 mouse model for DN) and were recruited

into the DN group and were given a high-fat diet for 12 weeks.<sup>20</sup> The control mice were fed with normal diet and were injected intraperitoneally with the same amount of sterile sodium citrate at the same pH as the DN model mice, and were given a normal diet for 12 weeks. After a duration of 12 weeks, euthanasia was performed and kidney tissue was collected from all mice involved in the experiment. Kidneys from 16 mice were harvested in this study, including ten mice in the DN group and six mice in the control group. Randomization was performed using a computer-generated schedule by a third-party.

### RNA Extraction and RT-qPCR

Total RNA was extracted from kidney tissue samples using the FastPure® Cell/Tissue Total RNA Isolation Kit V2 and quantified with a NanoDrop 2000 spectrophotometer (Thermo Fisher Scientific Inc). Subsequently, first-strand complementary DNA (cDNA) was synthesized from the total RNA employing the HiScript III RT SuperMix for qPCR (+gDNA wiper) reverse transcription kit. The cDNA was amplified using the ABI 7500 Fast Real-Time PCR system (Applied Biosystems, Foster City, CA, USA) and ChamQ Universal SYBR qPCR Master Mix. PCR was conducted with a temperature profile consisting of 40 cycles at 95°C for 30s, 95°C for 10s, and 60°C for 30s. The relative expression levels of the target mRNAs were normalized to the expression levels of glyceraldehyde-3-phosphate dehydrogenase (GAPDH) and analyzed utilizing the  $2^{-\Delta\Delta Ct}$  relative quantitative method. The PCR primer sequences are listed in Table 1.

### Statistical Analysis

Data from external datasets and animal experiments were statistically analyzed and visualized using GraphPad prism 9. The two sets of data from external datasets and animal experiments were initially tested for normality using the Shapiro–Wilk normality test. If the data did not follow a normal distribution, the Mann–Whitney test was performed. Conversely, if the data exhibited a normal distribution, the homogeneity test of variance was conducted. In cases where the variance was considered to be non-uniform, Welch’s *t*-test was employed, while a group *t*-test was used when the variance was uniform. Spearman correlation analysis was used for correlation analysis. All statistical analyses were two-tailed with  $P < 0.05$  were regarded statistically significant.

## Results

### Overview of the Study Design

The overall design scheme of our study is outlined in Figure 1. Firstly, We retrieved GSE142025 and GSE30528 from the GEO database based on the corresponding keywords and normalized the data from the two datasets. Next, we utilized the “limma” R packages to analyze DEGs. We then intersected the DEGs with PRGs and FRGs, resulting in 8 PFRDEGs. We performed GSEA functional enrichment analysis for all the genes in GSE142025 and further analyzed the 8 PFRDEGs using GO/KEGG, PPI study, and Cytoscape software, which led to the identification of hub PFRDEGs. Following we assessed the clinical significance of hub PFRDEGs, evaluated their potential role in diagnosing advanced DN, and validated them using external data and DN model mice. Finally, potential drug prediction for the treatment of advanced DN was performed based on the three hub PFRDEGs.

**Table 1** The PCR Primer Sequences

ID	Primer Name	Primer Sequence (5'–3')
14433	GAPDH	GACATGCCGCCTGGAGAAAC AGCCCAGGATGCCCTTTAGT
16819	LCN2	GCAGGTGGTACGTTGTGGG CTCTTGTAGCTCATAGATGGTGC
11450	ADIPOQ	GTTCCCAATGTACCCATTTCGC TGTTGCAGTAGAACTTGCCAG
13058	CYBB	CCCTTTGGTACAGCCAGTGAAGAT CAATCCCGGCTCCCACTAACATCA

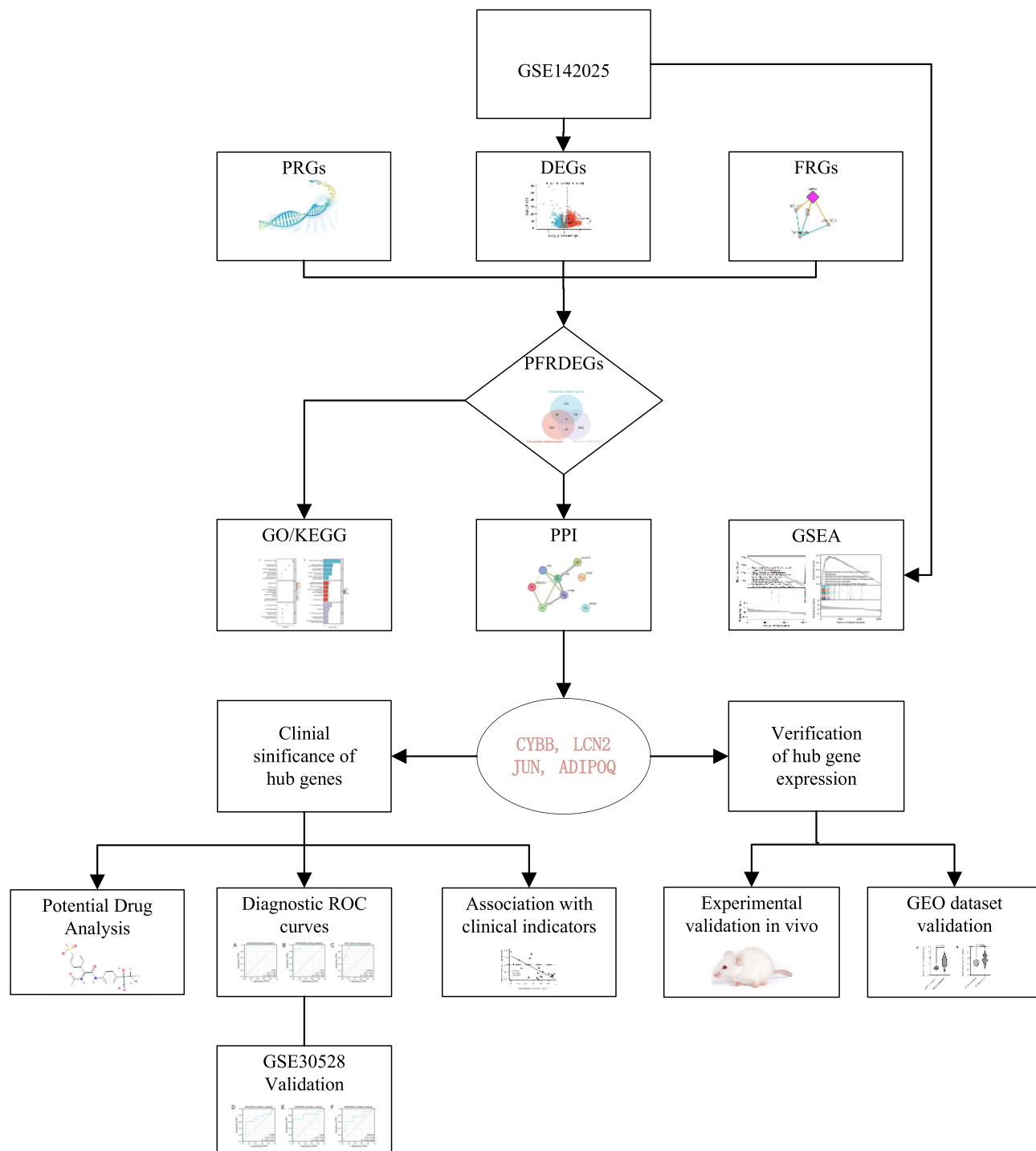


**Figure 1** Flowchart of research design and analyzing process of this study.

**Abbreviations:** DEGs, differentially expressed genes; PRGs, pyroptosis-related genes; FRGs, ferroptosis-related genes; PFRDEGs, Differentially Expressed Pyroptosis-and Ferroptosis- Related Genes; GEO, Gene Expression Omnibus; GO/KEGG, Gene Ontology Enrichment Analysis / Kyoto Encyclopedia of Genes and Genomes Pathway Analysis; PPI, protein-protein interaction; ROC, receiver operating characteristic.

## Identification of DEGs and the Landscape of the PFRDEGs

To identify the pathways and biological mechanisms related to advanced DN, we screened 1855 DEGs from GSE142025 microarray dataset based on the above selection criteria. Among these, 1037 genes were up-regulated and 818 were down-regulated (Figure 2A and B, Supplementary Table S5). Additionally, we screened 490 PRGs and 502 FRGs. By

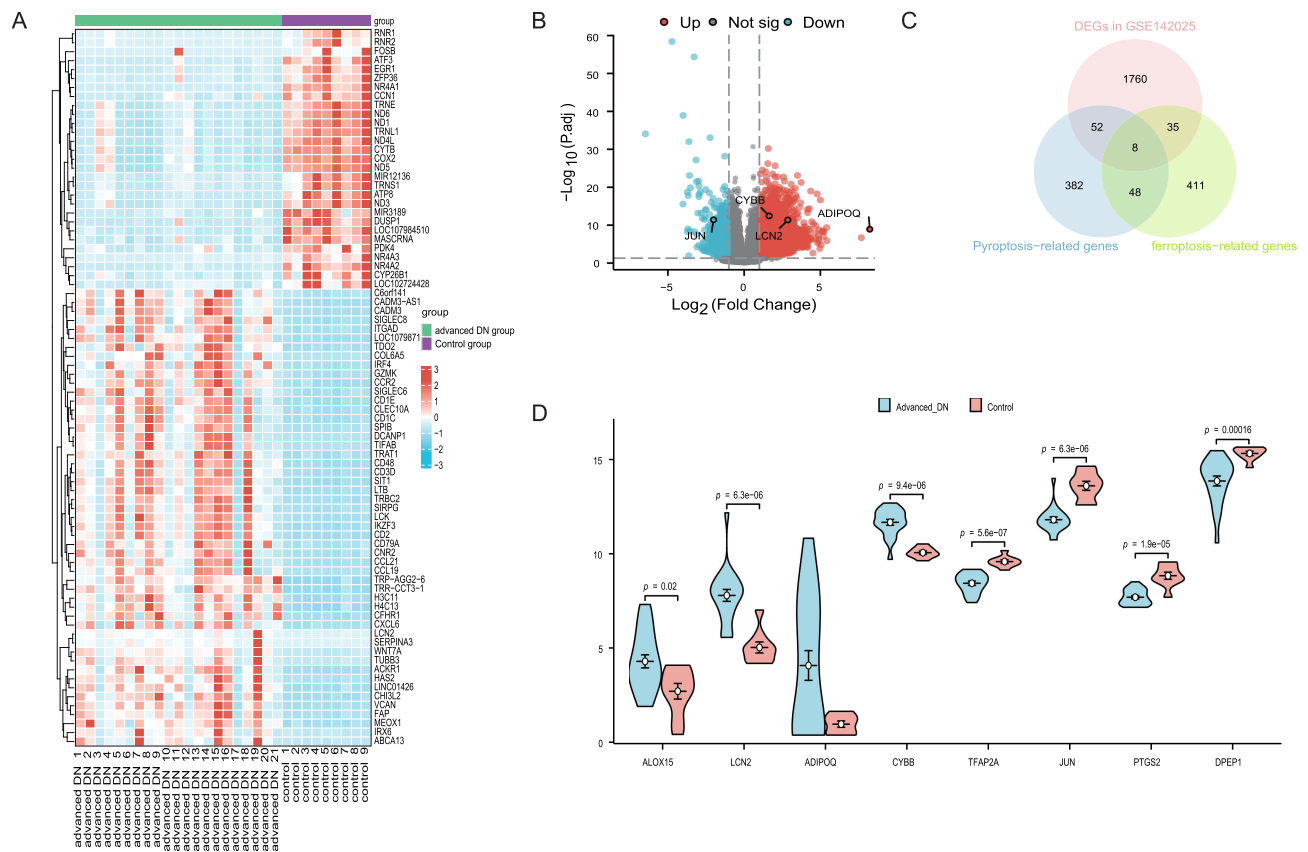


**Figure 2** Screening and identifying DEGs and PFRDEGs. **(A)** Heatmap of DEGs in GSE142025. The horizontal coordinates of the graph represent individual sample designations and the vertical coordinates represent gene names. **(B)** Volcano plot of DEGs in GSE142025. **(C)** Venn diagrams among DEGs, PRGs and FRGs. **(D)** Expression of the 8 PFRDEGs in the control and advanced DN groups. Blue and red represent advanced-DN group and control group, respectively.

intersecting the DEGs, PRGs and FRGs, we identified 8 PFRDEGs that exhibited significant differences between advanced DN patients and healthy controls (Figure 2C). These PFRDEGs include *JUN*, *CYBB*, *LCN2*, *DPEP1*, *ADIPOQ*, *ALOX15*, *PTGS2*, and *CGAS* (Figure 2D).

## Functional Enrichment Analysis

To delve into the function of PFRDEGs, GO/KEGG enrichment analyses were performed (Supplementary Table S6 present the results in detail). Firstly, biological features of PFRDEGs were explored through GO annotation: the main biological process (BP) enrichments of PFRDEGs included cellular response to metal ion (GO:0071248), regulation of smooth muscle cell proliferation (GO:0048660), positive regulation of cytokine production (GO:0001819), and so on. In terms of molecular function (MF), the major enrichments in PFRDEGs included R-SMAD binding (GO:0070412), cAMP response element binding (GO:0035497) and glycolipid binding (GO:0051861). Secondly, KEGG pathway analysis was conducted and the results showed that PFRDEGs were remarkably enriched in the IL-17 signaling pathway (hsa04657), AGE-RAGE signaling pathway in diabetic complications (hsa04933), and TNF signaling pathway (hsa04668) (Table 2, Figure 3A and B). Finally, to further investigate the potential pathways in DN, GSEA analyses were performed. The GSEA-enriched pathways mainly participated in oxidative phosphorylation, fcgr activation, fceri mediated NF-kb activation, and so on. Based on the NES value ranking, we selected the top 5 and bottom 5 pathway IDs, and the graphical representation of the results can be viewed in Figure 3C and D, Table 3. Supplementary Table S7 presents the results of GSEA in detail.

**Table 2** GO/KEGG Enrichment Analysis Results of PFRDEGs

Ontology	ID	Description	Gene Ratio	P. Adjust	q Value
BP	GO:0071248	Cellular response to metal ion	5/8	0.000	0.000
BP	GO:0031953	Negative regulation of protein autophosphorylation	2/8	0.001	0.000
BP	GO:0001819	Positive regulation of cytokine production	4/8	0.002	0.001
BP	GO:0048660	Regulation of smooth muscle cell proliferation	3/8	0.002	0.001
BP	GO:1903555	Regulation of tumor necrosis factor superfamily cytokine production	2/8	0.025	0.010
MF	GO:0016175	Superoxide-generating NAD(P)H oxidase activity	1/8	0.023	0.013
MF	GO:0035497	cAMP response element binding	1/8	0.030	0.016
MF	GO:0043027	Cysteine-type endopeptidase inhibitor activity involved in apoptotic process	1/8	0.035	0.019
MF	GO:0070412	R-SMAD binding	1/8	0.036	0.020
MF	GO:0051861	Glycolipid binding	1/8	0.042	0.023
KEGG	Hsa04657	IL-17 signaling pathway	3/7	0.002	0.002
KEGG	Hsa04216	Ferroptosis	2/7	0.015	0.011
KEGG	Hsa04933	AGE-RAGE signaling pathway in diabetic complications	2/7	0.038	0.028
KEGG	Hsa04625	C-type lectin receptor signaling pathway	2/7	0.038	0.028
KEGG	Hsa04668	TNF signaling pathway	2/7	0.038	0.028

### PPI Network Analysis for Identifying Hub Genes and Interactions Among Hub Genes

To obtain hub DEGs for a more in-depth analysis of the role of pyroptosis and ferroptosis in DN, PPI network of the PFRDEGs was constructed using the STRING online database. Out of the 8 PFRDEGs, 6 PFRDEGs were found to engage in dialogue with each other, while the remaining 2 PFRDEGs did not show any interaction (Figure 4A). The hub genes were identified using the MCODE-plugin in Cytoscape (Detailed parameters: Degree cutoff: 2; Cluster Finding: Haircut; Node Score Cutoff: 0.2; K-Core: 2; Max Depth: 100), including *JUN*, *LCN2*, *ADIPOQ* and *CYBB* (Figure 4B).

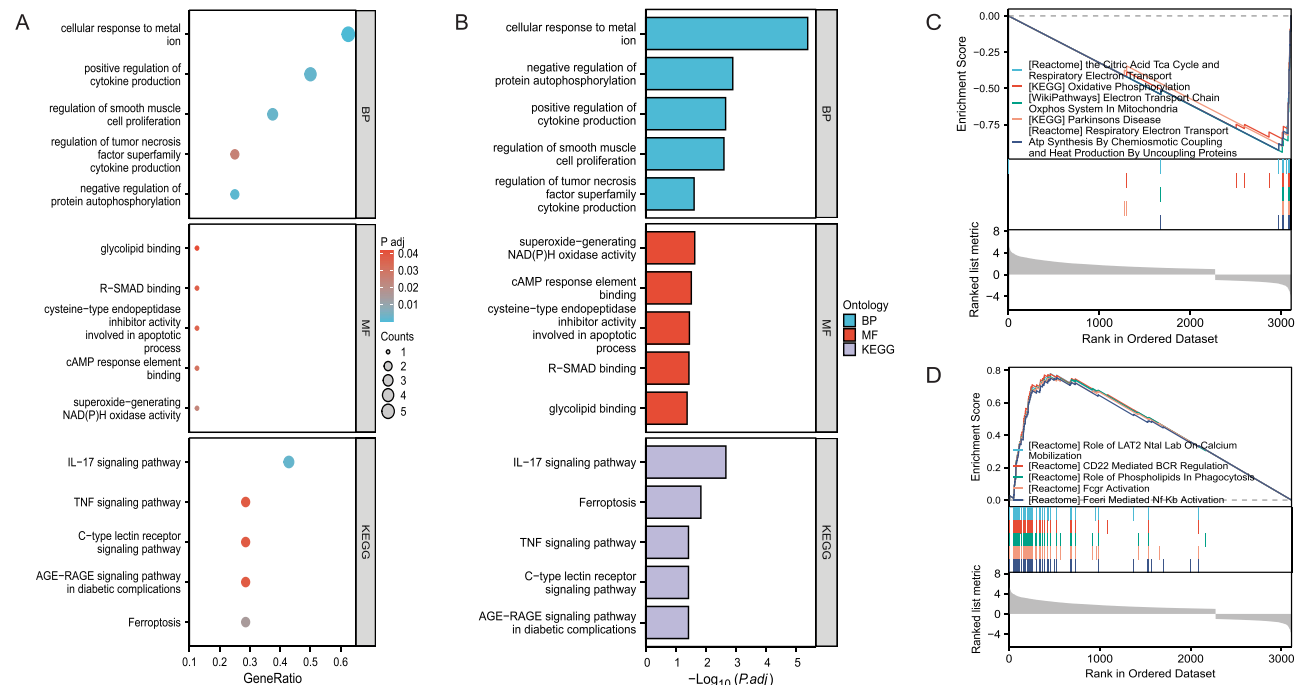


**Figure 3** GO/KEGG enrichment results of PFRDEGs and GSEA results of all the genes in GSE142025. **(A)** Bubble plot of the results of GO/KEGG enrichment analysis. **(B)** Histogram of the results of GO/KEGG enrichment analysis. **(C)** The graphical representation of the last 5 pathways in the GSEA results (The NES values are negative.). **(D)** The graphical representation of the The first 5 pathways in the GSEA results (The NES values are positive.).



**Table 3** GSEA Results

ID	NES	P. Adjust	q Value
Reactome_the_citric_acid_tca_cycle_and_respiratory_electron_transport	-4.220	0.000	0.000
Kegg_oxidative_phosphorylation	-4.143	0.000	0.000
Wp_electron_transport_chain_oxphos_system_in_mitochondria	-4.119	0.000	0.000
Kegg_parkinsons_disease	-4.080	0.000	0.000
Reactome_respiratory_electron_transport_atp_synthesis_by_chemiosmotic_coupling_and_heat_production_by_uncoupling_proteins	-4.059	0.000	0.000
Reactome_role_of_lat2_ntal_lab_on_calcium_mobilization	3.749	0.000	0.000
Reactome_cd22_mediated_bcr_regulation	3.739	0.000	0.000
Reactome_role_of_phospholipids_in_phagocytosis	3.692	0.000	0.000
Reactome_fcgr_activation	3.680	0.000	0.000
Reactome_fceri_mediated_nf_kb_activation	3.676	0.000	0.000

To gain further insights into the intermolecular interaction of these hub genes, the study utilized GeneMANIA online software to search for related genes, resulting in the identification of 20 genes with a total of 425 links (Figure 4C).

### Immune Infiltration Analysis and Correlations Between Hub Genes and Immune Cells

The CIBERSORTx algorithm has been applied to investigate the landscape of immune infiltration in advanced DN. The boxplots of 22 immune cell types between advanced DN group and Control group are shown in Figure 5A, [Supplementary Table S8](#).

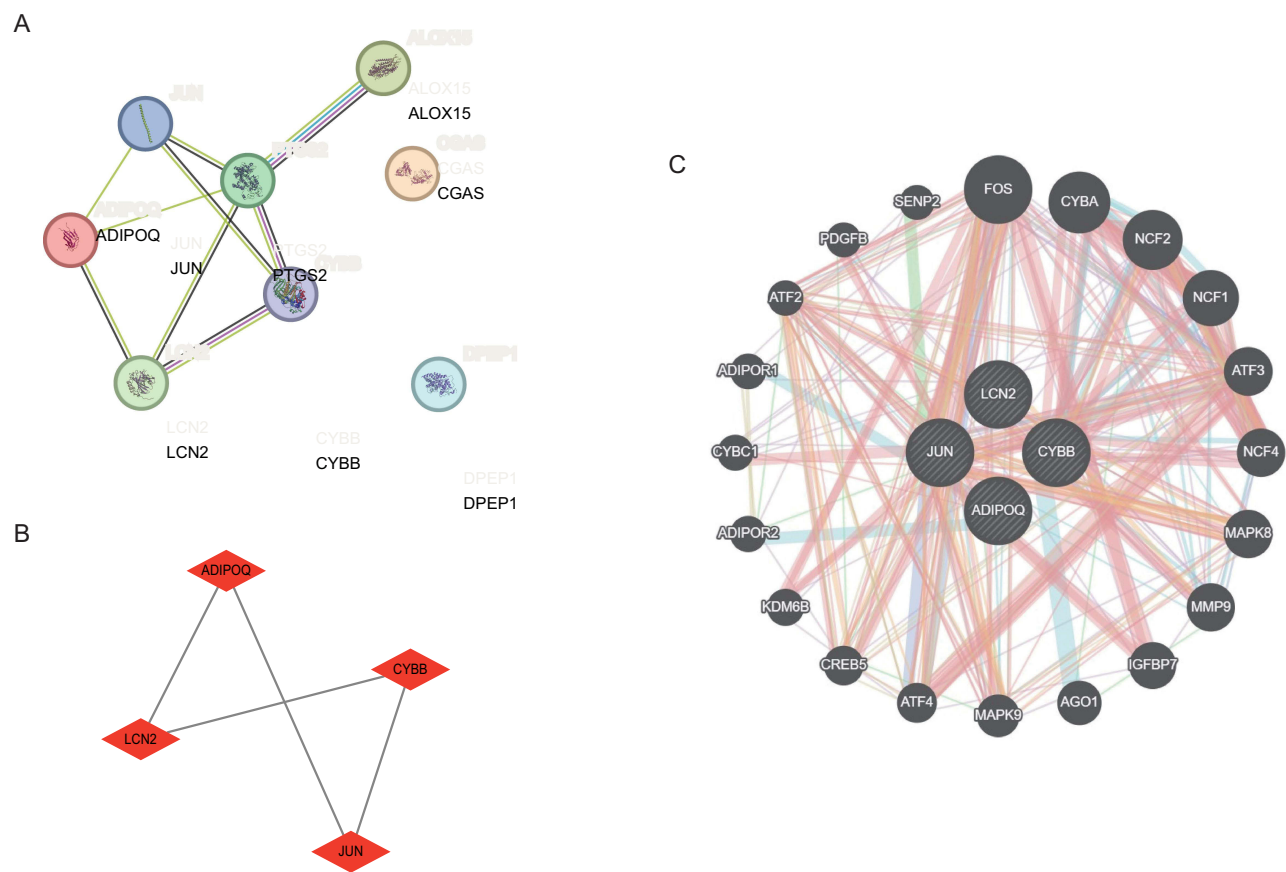


**Figure 4** PPI network among proteins encoded by PFRDEGs and prediction of intermolecular interactions of the hub genes. **(A)** PPI network analysis of proteins encoded by PFRDEGs. **(B)** The four hub genes were identified using the MCODE-plugin of Cytoscape software. **(C)** Prediction of intermolecular interactions of the hub genes. (The purple line means that the two proteins are co-expressed, the yellow line means that the two proteins are shared protein domains, the pink line means that the two proteins are physical interactions, the blue line means that the two proteins are co-localisation, the Orange line means that the two proteins are predicted.).

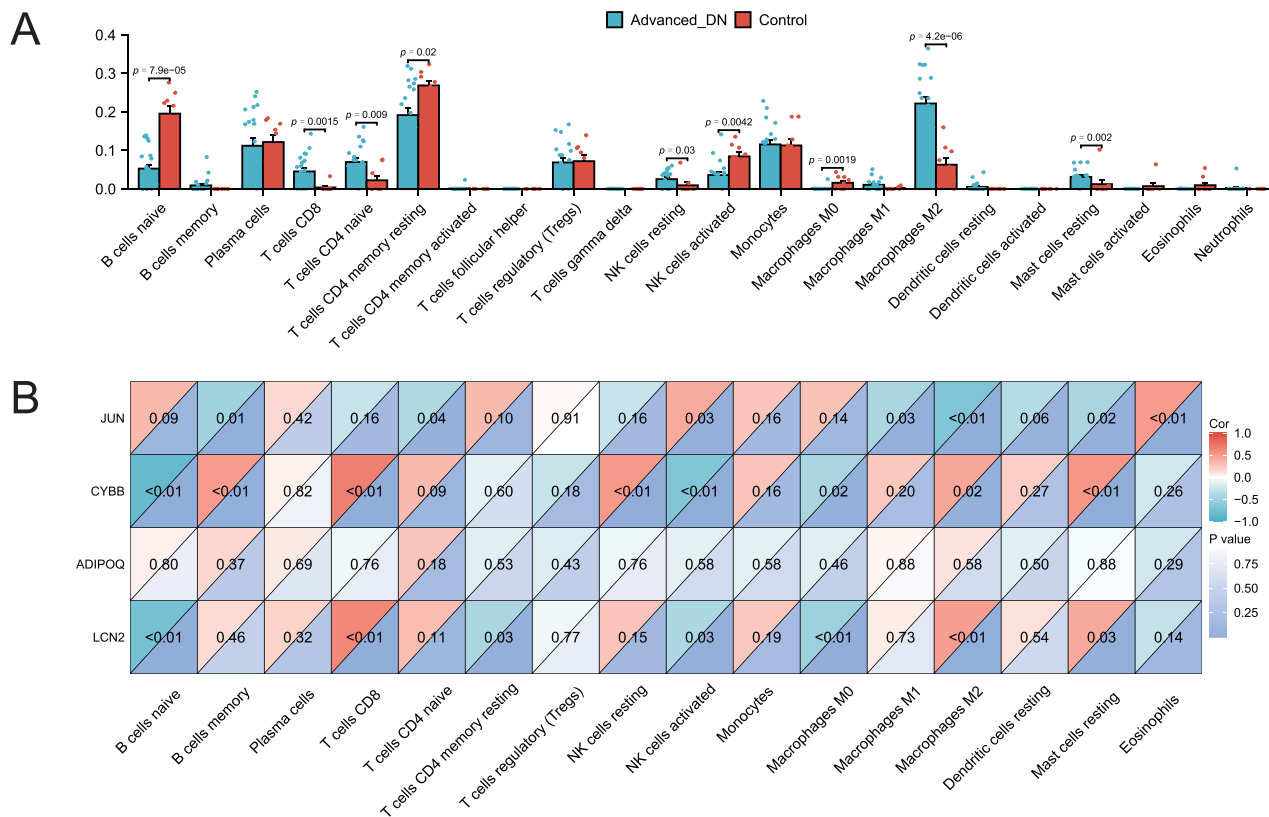


**Figure 5** Immune infiltration analysis. (A) The boxplots of 22 immune cells between advanced DN samples and control samples. (B) Correlation between each of the immune cells and four hub genes.

Specifically, the types of immune cells in advanced DN were B cells naive, T cells CD8, T cells CD4 naive, T cells CD4 memory resting, NK cells activated, Macrophages M0, Macrophages M2 and Mast cells resting. In addition, we analyzed the correlation between each immune cell and the four hub genes. As shown in Figure 5B, Supplementary Table S9, JUN expression was associated with B cells memory, T cells CD4 naive, Macrophages M2, Mast cells resting; CYBB expression was associated with B cells naive, B cells memory, T cells CD8, NK cells resting, NK cells activated, Macrophages M0, Macrophages M2, and Mast cells resting; LCN2 expression was associated with B cells naive, T cells CD8, T cells CD4 memory resting, NK cells activated, Macrophages M0, Macrophages M2 and Mast cells resting. In summary, these results suggest that JUN, LCN2 and CYBB may contribute to the immune microenvironment of advanced DN.

## Validation of Hub Genes in External Datasets

To visually compare the differences in hub genes expression between the advanced DN group and the control group, we used violin plots. As shown in Figure 6A, *CYBB* and *LCN2* in GSE142025 were significantly upregulated, *JUN* was significantly downregulated in the advanced DN group compared with the control group. To validate the reliability of the four hub genes, we verified the expression of these genes in the GSE30528 dataset. As shown in Figure 6B, *CYBB* and *LCN2* in this dataset were significantly upregulated in DN group compared with the control group. In summary, only *CYBB* and *LCN2* were discrepant in both external datasets.

## Hub Genes (*CYBB*, *LCN2* and *ADIPOQ*) Have Potential Diagnostic Power

To evaluate the diagnostic efficacy of the four hub genes identified in the previous analysis, ROC curves were generated and the AUC value was used to evaluate their effectiveness in diagnosing advanced DN. The diagnostic efficacy of three hub genes (*CYBB*, *LCN2* and *ADIPOQ*) was found to be superior. Figure 7A–C provides an overview of the ROC curves for the three hub genes, showing that the AUC for *CYBB* was 0.952 (95% CI, 0.859–1.000;  $P = 0.0003$ ); AUC for *LCN2*

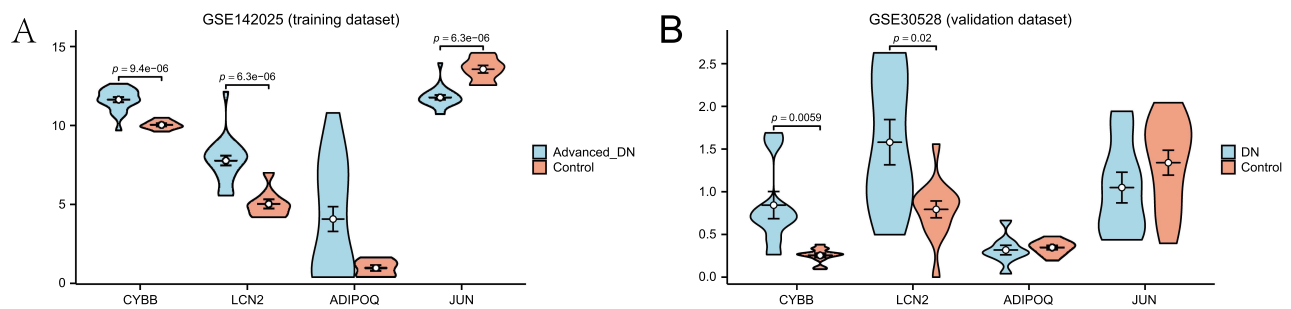


**Figure 6** The expression of hub genes in GSE142025 and validation in the external datasets. **(A)** The expression of CYBB, LCN2, ADIPOQ and JUN in GSE142025. **(B)** The expression of CYBB, LCN2, ADIPOQ and JUN in GSE30528 (validation dataset).

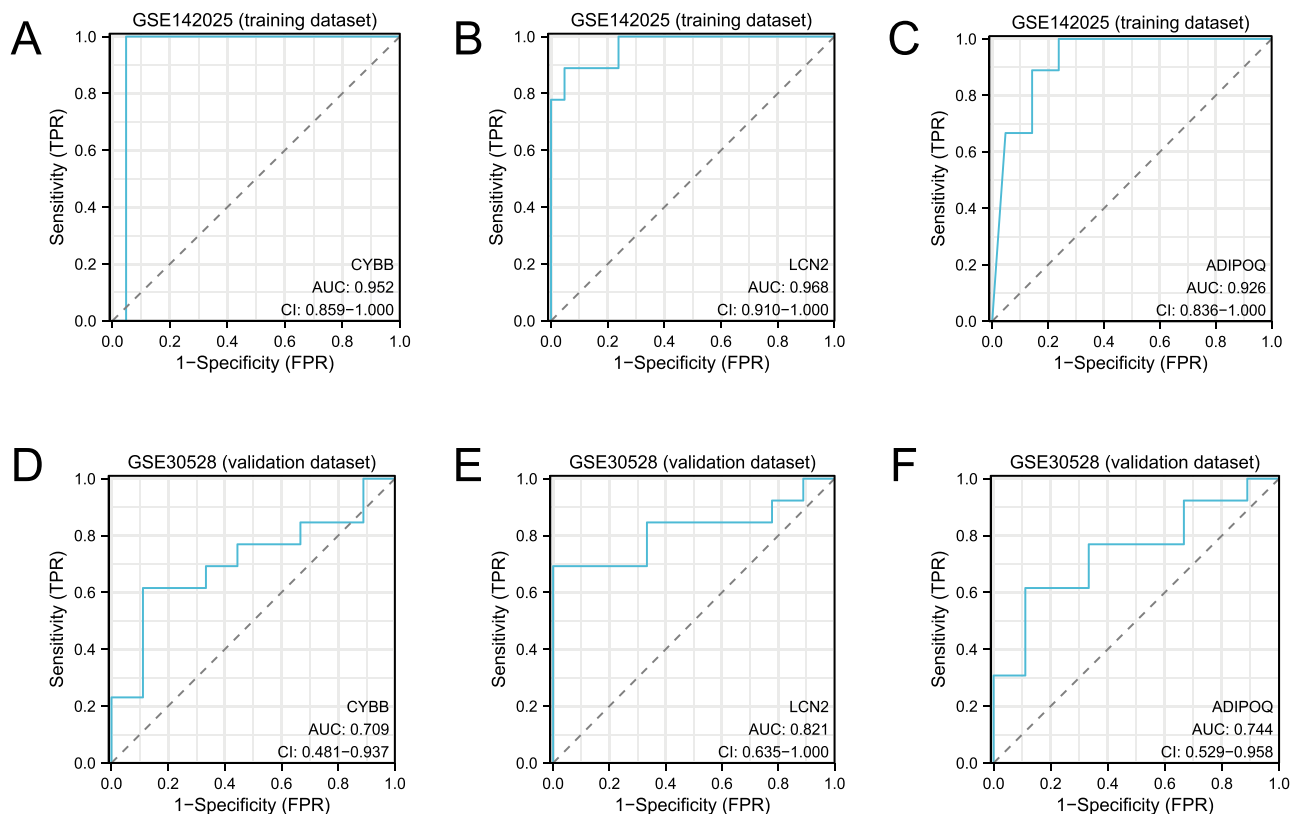


**Figure 7** Diagnostic value of the hub genes with ROC curves and validation in external dataset. **(A–C)** ROC curve analysis of the hub genes in the GSE142025. **(D–F)** Validation of the diagnostic value of the hub genes in the GSE30528.

was 0.968 (95% CI, 0.910–1.000;  $P = 0.009$ ), and AUC for *ADIPOQ* was 0.926 (95% CI, 0.836–1.000;  $P = 0.0034$ ). This diagnostic efficacy of the three genes was further confirmed in the GSE30528 dataset and the AUC was 0.709 (95% CI, 0.481–0.937), 0.821 (95% CI, 0.635–1.000) and 0.744 (95% CI, 0.529–0.958) for *CYBB*, *LCN2* and *ADIPOQ*, respectively (Figure 7D–F). These findings demonstrate that these hub genes may play a significant role in the pathological mechanisms underlying DN.

## Expression of *CYBB* and *LCN2* Was Significantly Higher in DN Group and Negatively Correlated with eGFR

The aforementioned findings indicate that *CYBB*, *LCN2* and *ADIPOQ* have potential diagnostic value. To further validate the reliability of the data obtained from this bioinformatics analysis, we verified the expression of *CYBB* and *LCN2* by

cross-referencing it with data from Nephroseq V5 database. The results obtained by querying Nephroseq V5 database showed that in DN patients, the expression of *CYBB* and *LCN2* was significantly higher than that of healthy living donors [ $P = 0.0022$  (Figure 8A);<sup>40</sup>  $P < 0.0001$  (Figure 8B)<sup>40</sup>]; Moreover, the expression of *Cybb* and *Lcn2* was also significantly up-regulated in DN mice [ $P = 0.0142$  (Figure 8C);<sup>41</sup>  $P < 0.0001$  (Figure 8D)<sup>41</sup>]. To further explore the clinical significance of the three genes, we performed a correlation analysis between the three genes and eGFR, because eGFR is a crucial impact factor on the prognosis of DN. The results showed that the expression of *CYBB* was negatively correlated with eGFR [ $r = -0.7061$ ,  $P = 0.0002$ ],<sup>42</sup> Figure 8E], the expression of *LCN2* was negatively correlated with eGFR [ $r = -0.7588$ ,  $P = 0.0068$ ],<sup>42</sup> Figure 8F]. These findings suggest that the expression of *LCN2* and *CYBB* can be utilized to a certain extent for predicting renal function in DN.

## The Expression of the *Cybb* and *Lcn2* is Markedly Elevated in C57BL/6 Mice Models for DN

Efficacy are key requirement for the translation of any new biomarkers to the clinic. In order to further validate the data obtained in the bioinformatics analysis, a series of biological experiments were conducted, including animal experiments and molecular biology experiments. mRNA expression of the hub genes in the kidney of C57BL/6 mice were measured using RT-qPCR. As depicted in Figure 9, when compared to the control group, the mRNA expression of *Cybb* and *Lcn2* were significantly higher expression in the DN group (*Cybb*:  $1.310 \pm 0.417$ ,  $p = 0.0022$ ; *Lcn2*:  $1.921 \pm 0.592$ ,  $p = 0.0078$ ). However, there were no statistically differences in the expression of *Jun* and *Adipoq* between the two groups.

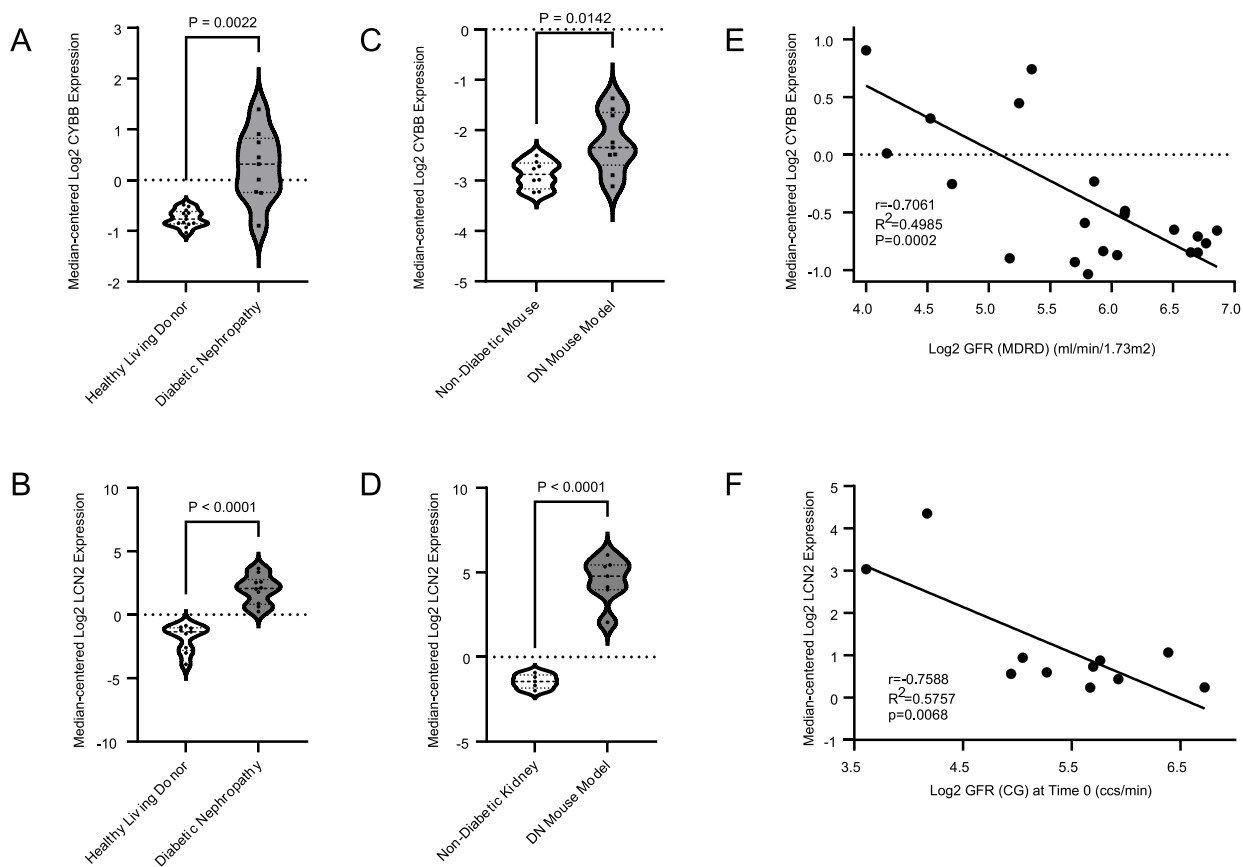


**Figure 8** Expression of *CYBB* and *LCN2* was significantly higher in DN group and negatively correlated with eGFR in external datasets. (A and B) Expression of *CYBB* and *LCN2* was significantly higher in DN patients. (C and D) Expression of *Cybb* and *Lcn2* was significantly higher in DN mice. (E and F) The expression of *CYBB* and *LCN2* was negatively correlated with eGFR in DN patients.

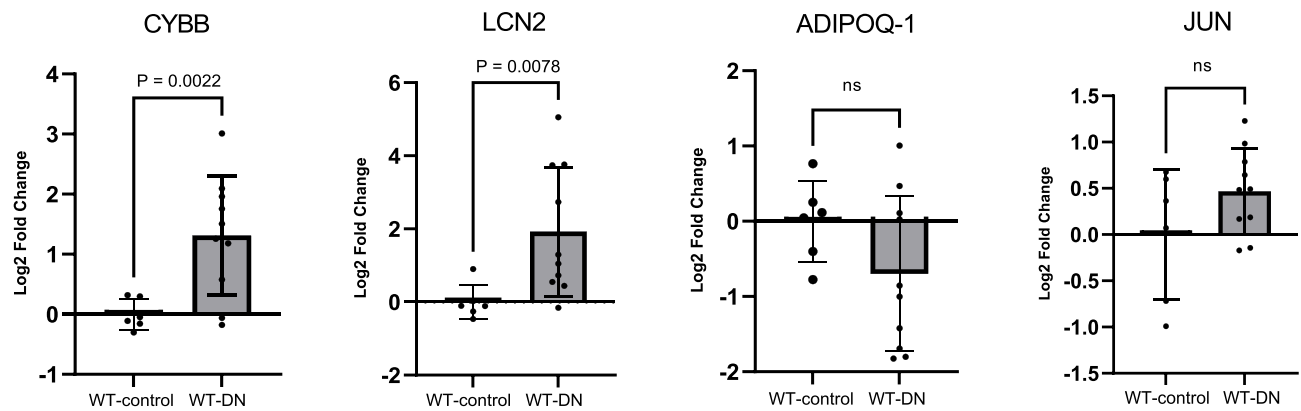


**Figure 9** Validation of the hub genes in C57BL/6 mice models for DN. The mRNA expression of the four hub genes in C57BL/6 mice models for DN were determined by RT-qPCR assay. (control group: n =6, DN group: n=10).

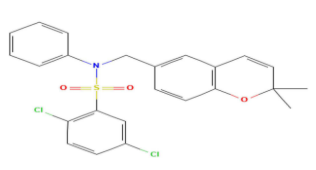
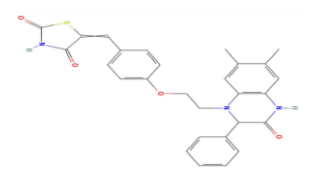
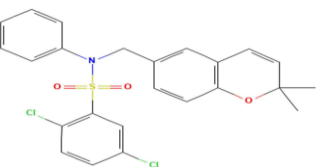
## Prediction of Marker Gene-Targeted Therapeutic Agents

The another primary aim of this study is to forecast potential therapeutic agents that could be effective in treating advanced DN. To achieve this, the ChEMBL database was thoroughly investigated, and three therapeutic agents—CHEMBL420360, CHEMBL182828, and CHEMBL1823903—were identified as targeting the aforementioned hub genes (Table 4). This discovery offers a robust foundation of both experimental and theoretical evidence to support the development of precision treatments for advanced DN.

## Discussion

As a prevalent and recurring microvascular complication of diabetes mellitus, DN has emerged as a significant contributor to ESKD and a public health challenge worldwide.<sup>43</sup> Studies have shown that ferroptosis and pyroptosis can cause renal damage through corresponding pathways, and inhibition of ferroptosis and pyroptosis, respectively, can prevent or delay renal damage and renal fibrosis. Multiple studies have demonstrated the existence of numerous interconnections between pyroptosis and ferroptosis, encompassing shared triggers, molecular components, and protective mechanisms.<sup>23</sup> More importantly, many recent studies have found that there is a mechanistic crosstalk between pyroptosis and ferroptosis, which provides new perspectives on the mechanistic study of the disease and new avenues for

**Table 4** Potential Therapeutic Agents List

Compound ID	Molecular Formula	2D Structure
CHEMBL420360	C <sub>19</sub> H <sub>27</sub> N <sub>5</sub> O <sub>4</sub>	
CHEMBL182828	C <sub>28</sub> H <sub>25</sub> N <sub>3</sub> O <sub>4</sub> S	
CHEMBL1823903	C <sub>24</sub> H <sub>21</sub> Cl <sub>2</sub> N <sub>3</sub> O <sub>3</sub> S	

the treatment of the disease.<sup>28–31</sup> Consequently, in this study, we conducted the combined study of ferroptosis and pyroptosis in advanced DN by means of bioinformatics.

Initially, we identified eight PFRDEGs. Subsequently, We conducted GO/KEGG enrichment analysis on the 8 PFRDEGs and GSEA on all genes in GSE142025. The GO analysis revealed that the PFRDEGs were primarily involved in positive regulation of cytokine production, regulation of smooth muscle cell proliferation, cellular response to metal ion, and so on. The KEGG enrichment analysis showed that the PFRDEGs were enriched in the IL-17 signaling pathway, AGE-RAGE signaling pathway in diabetic complications, and TNF signaling pathway. Additionally, we conducted GSEA, which mainly participated in oxidative phosphorylation, fcgr activation, fceri mediated NF-kb activation, and so on. Subsequently, four hub PFRDEGs (*JUN*, *CYBB*, *LCN2*, and *ADIPOQ*) were selected, and the three hub PFRDEGs—*CYBB*, *LCN2*, and *ADIPOQ* were up-regulated while *JUN* was down-regulated. To further explore the clinical significance of hub PFRDEGs, we assessed the diagnostic value of the hub PFRDEGs and did a correlation analysis between these hub PFRDEGs and clinical indicators. We found that *CYBB*, *LCN2*, and *ADIPOQ* exhibited high accuracy (all AUC>0.9) in predicting DN and expression of *CYBB* and *LCN2* was negatively correlated with eGFR. Additionally, we also mined three therapeutic agents targeting *CYBB*, *LCN2*, and *ADIPOQ*. These findings suggest that *CYBB*, *LCN2*, and *ADIPOQ* play a significant role in diagnosing advanced DN, and provide a theoretical basis for the precise treatment for advanced DN.

In our study, we found that *CYBB* could be considered as a potential biomarker for advanced DN. *CYBB*, also known as Cytochrome b-245 beta chain, encodes the gp91phox protein. Mutations in this gene are associated with X-linked chronic granulomatous disease.<sup>44</sup> Despite the fact that reports on this gene's involvement in DN are limited, our study found that *Cybb* expression was significantly overexpressed in renal tissues of DN mice (p=0.0022), which aligns with the only literature results.<sup>45</sup> The role of *CYBB* in DN remains unclear due to the limited number of studies, but our discovery of the *CYBB* can provide valuable insights for the diagnostic markers of DN in future research.

In addition, *ADIPOQ* (adiponectin), a protein secreted by adipose tissue, is deemed to be an endogenous insulin sensitizer. *ADIPOQ* exhibits anti-inflammatory and antiatherogenic effects, and regulates glucose and lipid metabolism as well as insulin action.<sup>46</sup> Abnormal levels of serum adiponectin have been correlated with T2DM, insulin resistance, obesity, cardiovascular diseases, and nephropathy.<sup>47</sup> In our in vivo experiment, we did not observe a significant difference in *ADIPOQ* expression compared to the control group. The exact mechanism of *ADIPOQ*'s role in DN has not been extensively studied and requires further research.

Furthermore, *LCN2*, also known as neutrophil gelatinase-associated lipocalin (NGAL), is a transporter protein expressed in a wide range of cells. During acute kidney injury, *LCN2* is secreted in high amounts into the urine and blood by tubular cells even before serum creatinine levels increase.<sup>48</sup> In individuals with type 1 diabetes mellitus, *LCN2* concentration is elevated in both blood and urine samples prior to the presence of microalbuminuria.<sup>49</sup> Studies have shown a positive correlation between *LCN2* and albumin excretion rate as well as hemoglobin A1c levels.<sup>50,51</sup> In patients with T2DM, high expression of *LCN2* serves as a strong predictor of GFR impairment. We further found the meaningful value of *LCN2* in the diagnosis of advanced DN by a joint of bioinformatics analysis and biological experiments based on previous literature. Therefore, *LCN2* is expected to serve as a potential biomarker for advanced DN.

However, this study has several limitations. The evidence is based on publicly available data, and although we have performed expression validation with another dataset and validated in vivo in mice, further experiments are needed to validate the three diagnostic markers before they can be applied to the clinic.

In summary, we applied bioinformatics methods to jointly conduct in-depth data mining of the dataset of advanced DN from two perspectives, namely ferroptosis and pyroptosis, and found that *CYBB*, *LCN2* and *ADIPOQ* have potential diagnostic and targeted therapeutic value. This study is expected to provide constructive reference and basis for clinical detection and targeted therapy of advanced DN.

## Conclusions

Our study identified *CYBB*, *LCN2*, and *ADIPOQ* as potential biomarkers for advanced DN by utilizing bioinformatics analysis of disease databases. Furthermore, our research validated the diagnostic value of *Cybb* and *Lcn2* through animal experiments. Additionally, we discovered three small molecule drugs via drug screening that show promise for targeted

treatment of advanced DN. These findings not only provide new insights into the role of pyroptosis and ferroptosis in advanced DN, but also lay the foundation for future research into non-invasive diagnostic markers and precision therapies for advanced DN.

## Author Contributions

All authors made a significant contribution to the work reported, whether that is in the conception, study design, execution, acquisition of data, analysis and interpretation, or in all these areas; took part in drafting, revising or critically reviewing the article; gave final approval of the version to be published; have agreed on the journal to which the article has been submitted; and agree to be accountable for all aspects of the work.

## Funding

This work is supported by the Senior Integrated Chinese and Western Medicine Talent Training Program in Shanghai, China [ZY (2018–2020)-RCPY-2020].

## Disclosure

The authors declare no competing interests in this work.

## References

1. Himmelfarb J, Tuttle KR. New therapies for diabetic kidney disease. *N Engl J Med*. 2013;369(26):2549–2550. doi:10.1056/NEJMe1313104
2. Wang X, Jiang L, Liu XQ, et al. Identification of Genes Reveals the Mechanism of Cell Ferroptosis in Diabetic Nephropathy. *Front Physiol*. 2022;13(890566). doi:10.3389/fphys.2022.890566
3. Afkarian M, Sachs MC, Kestenbaum B, et al. Kidney disease and increased mortality risk in type 2 diabetes. *J Am Soc Nephrol*. 2013;24(2):302–308. doi:10.1681/ASN.2012070718
4. Jiao F, Wong CKH, Tang SCW, et al. Annual direct medical costs associated with diabetes-related complications in the event year and in subsequent years in Hong Kong. *Diabetic Med*. 2017;34(9):1276–1283. doi:10.1111/dme.13416
5. Fan Y, Yi Z, D'Agati VD, et al. Comparison of Kidney Transcriptomic Profiles of Early and Advanced Diabetic Nephropathy Reveals Potential New Mechanisms for Disease Progression. *Diabetes*. 2019;68(12):2301–2314. doi:10.2337/db19-0204
6. Molitch ME, Steffes M, Sun W, et al. Development and progression of renal insufficiency with and without albuminuria in adults with type 1 diabetes in the diabetes control and complications trial and the epidemiology of diabetes interventions and complications study. *Diabetes Care*. 2010;33(7):1536–1543. doi:10.2337/dc09-1098
7. Parving HH, Gall MA, Skott P, et al. Prevalence and causes of albuminuria in non-insulin-dependent diabetic patients. *Kidney Int*. 1992;41(4):758–762. doi:10.1038/ki.1992.118
8. Caramori ML, Fioretto P, Mauer M. Low glomerular filtration rate in normoalbuminuric type 1 diabetic patients: an indicator of more advanced glomerular lesions. *Diabetes*. 2003;52(4):1036–1040. doi:10.2337/diabetes.52.4.1036
9. Fioretto P, Mauer M, Carraro A, et al. Renal structural changes in non-insulin-dependent diabetes mellitus. *Am J Hypertens*. 1997;10(9 Pt 2):184S–188S. doi:10.1016/s0895-7061(97)00151-9
10. Macisaac RJ, Ekinci EI, Jerums G. Markers of and risk factors for the development and progression of diabetic kidney disease. *Am J Kidney Dis*. 2014;63(2 Suppl 2):S39–62. doi:10.1053/j.ajkd.2013.10.048
11. Lin J, Cheng A, Cheng K, et al. New Insights into the Mechanisms of Pyroptosis and Implications for Diabetic Kidney Disease. *Int J Mol Sci*. 2020;21(19):7057. doi:10.3390/ijms21197057
12. Erekat NS. Programmed Cell Death in Diabetic Nephropathy: a Review of Apoptosis, Autophagy, and Necroptosis. *Medical Sci Monit*. 2022;28:e937766. doi:10.12659/MSM.937766
13. Dixon SJ, Lemberg KM, Lamprecht MR, et al. Ferroptosis: an iron-dependent form of nonapoptotic cell death. *Cell*. 2012;149(5):1060–1072. doi:10.1016/j.cell.2012.03.042
14. Feng Q, Yang Y, Ren K, et al. Broadening horizons: the multifaceted functions of ferroptosis in kidney diseases. *Int J Bio Sci*. 2023;19(12):3726–3743. doi:10.7150/ijbs.85674
15. Li S, Zheng L, Zhang J, et al. Inhibition of ferroptosis by up-regulating Nrf2 delayed the progression of diabetic nephropathy. *Free Radic Biol Med*. 2021;162:435–449. doi:10.1016/j.freeradbiomed.2020.10.323
16. Wang H, Liu D, Zheng B, et al. Emerging Role of Ferroptosis in Diabetic Kidney Disease: molecular Mechanisms and Therapeutic Opportunities. *Int J Bio Sci*. 2023;19(9):2678–2694. doi:10.7150/ijbs.81892
17. Zuo Y, Chen L, Gu H, et al. GSDMD-mediated pyroptosis: a critical mechanism of diabetic nephropathy. *Expert Rev Mol Med*. 2021;23:e23. doi:10.1017/erm.2021.27
18. Qu X, Zhai B, Liu Y, et al. Pyrroloquinoline quinone ameliorates renal fibrosis in diabetic nephropathy by inhibiting the pyroptosis pathway in C57BL/6 mice and human kidney 2 cells. *Biomed Pharmacother*. 2022;150(112998):112998. doi:10.1016/j.biopha.2022.112998
19. Shen Y, Chen W, Lin K, et al. Notoginsenoside Fc, a novel renoprotective agent, ameliorates glomerular endothelial cells pyroptosis and mitochondrial dysfunction in diabetic nephropathy through regulating HMGCS2 pathway. *Phytomedicine*. 2024;126(155445):155445. doi:10.1016/j.phymed.2024.155445
20. Cheng Q, Pan J, Zhou ZL, et al. Caspase-11/4 and gasdermin D-mediated pyroptosis contributes to podocyte injury in mouse diabetic nephropathy. *Acta Pharmacol Sin*. 2021;42(6):954–963. doi:10.1038/s41401-020-00525-z

21. Zhu W, Li YY, Zeng HX, et al. Carnosine alleviates podocyte injury in diabetic nephropathy by targeting caspase-1-mediated pyroptosis. *Int Immunopharmacol.* 2021;101(Pt B):108236. doi:10.1016/j.intimp.2021.108236
22. Han J, Zuo Z, Shi X, et al. Hirudin ameliorates diabetic nephropathy by inhibiting Gsdmd-mediated pyroptosis. *Cell Biol Toxicol.* 2023;39(3):573–589. doi:10.1007/s10565-021-09622-z
23. Sanz AB, Sanchez-Nino MD, Ramos AM, et al. Regulated cell death pathways in kidney disease. *Nat Rev Nephrol.* 2023;19(5):281–299. doi:10.1038/s41581-023-00694-0
24. Tang R, Xu J, Zhang B, et al. Ferroptosis, necroptosis, and pyroptosis in anticancer immunity. *J Hematol Oncol.* 2020;13(1):110. doi:10.1186/s13045-020-00946-7
25. Xu L. Crosstalk of three novel types of programmed cell death defines distinct microenvironment characterization and pharmacogenomic landscape in breast cancer. *Front Immunol.* 2022;13(942765). doi:10.3389/fimmu.2022.942765
26. Yang Z, Shi J, Chen L, et al. Role of Pyroptosis and Ferroptosis in the Progression of Atherosclerotic Plaques. *Front Cell Dev Biol.* 2022;10(811196). doi:10.3389/fcell.2022.811196
27. Yang J, Hu S, Bian Y, et al. Targeting Cell Death: pyroptosis, Ferroptosis, Apoptosis and Necroptosis in Osteoarthritis. *Front Cell Dev Biol.* 2021;9(789948). doi:10.3389/fcell.2021.789948
28. Zhou S, Liu J, Wan A, et al. Epigenetic regulation of diverse cell death modalities in cancer: a focus on pyroptosis, ferroptosis, cuproptosis, and disulfidoptosis. *J Hematol Oncol.* 2024;17(1):22. doi:10.1186/s13045-024-01545-6
29. Wan S, Zhang G, Liu R, et al. Pyroptosis, ferroptosis, and autophagy cross-talk in glioblastoma opens up new avenues for glioblastoma treatment. *Cell Commun Signal.* 2023;21(1):115. doi:10.1186/s12964-023-01108-1
30. Zhang L, Hu Z, Li Z, et al. Crosstalk among mitophagy, pyroptosis, ferroptosis, and necroptosis in central nervous system injuries. *Neural Regen Res.* 2024;19(8):1660–1670. doi:10.4103/1673-5374.389361
31. Cao Z, Qin H, Huang Y, et al. Crosstalk of pyroptosis, ferroptosis, and mitochondrial aldehyde dehydrogenase 2-related mechanisms in sepsis-induced lung injury in a mouse model. *Bioengineered.* 2022;13(3):4810–4820. doi:10.1080/21655979.2022.2033381
32. Fan Y, Yi Z, D'Agati VD, et al. Erratum. Comparison of Kidney Transcriptomic Profiles of Early and Advanced Diabetic Nephropathy Reveals Potential New Mechanisms for Disease Progression. *Diabetes.* 2020;69(4):797. doi:10.2337/db20-er04b
33. Woroniecka KI, Park AS, Mohtat D, et al. Transcriptome analysis of human diabetic kidney disease. *Diabetes.* 2011;60(9):2354–2369. doi:10.2337/db10-1181
34. Na J, Sweetwyne MT, Park AS, et al. Diet-Induced Podocyte Dysfunction in Drosophila and Mammals. *Cell Rep.* 2015;12(4):636–647. doi:10.1016/j.celrep.2015.06.056
35. Wang J, Wang Z, Jia W, et al. The role of costimulatory molecules in glioma biology and immune microenvironment. *Front Genetics.* 2022;13(1024922). doi:10.3389/fgene.2022.1024922
36. Guo Q, Zhao L, Yan N, et al. Integrated pan-cancer analysis and experimental verification of the roles of tropomyosin 4 in gastric cancer. *Front Immunol.* 2023;14(1148056). doi:10.3389/fimmu.2023.1148056
37. Szklarczyk D, Gable AL, Lyon D, et al. STRING v11: protein-protein association networks with increased coverage, supporting functional discovery in genome-wide experimental datasets. *Nucleic Acids Res.* 2019;47(D1):D607–D613. doi:10.1093/nar/gky1131
38. Meng Z, Chen Y, Wu W, et al. Exploring the Immune Infiltration Landscape and M2 Macrophage-Related Biomarkers of Proliferative Diabetic Retinopathy. *Front Endocrinol.* 2022;13(841813). doi:10.3389/fendo.2022.841813
39. Lay AC, Hale LJ, Stowell-Connolly H, et al. IGFBP-1 expression is reduced in human type 2 diabetic glomeruli and modulates  $\beta$ 1-integrin/FAK signalling in human podocytes. *Diabetologia.* 2021;64(7):1690–1702. doi:10.1007/s00125-021-05427-1
40. Ju W, Nair V, Smith S, et al. Tissue transcriptome-driven identification of epidermal growth factor as a chronic kidney disease biomarker. *Sci, trans med.* 2015;7(316):316ra193. doi:10.1126/scitranslmed.aac7071
41. Hodgins JB, Nair V, Zhang H, et al. Identification of cross-species shared transcriptional networks of diabetic nephropathy in human and mouse glomeruli. *Diabetes.* 2013;62(1):299–308. doi:10.2337/db11-1667
42. Schmid H, Boucherot A, Yasuda Y, et al. Modular activation of nuclear factor-kappaB transcriptional programs in human diabetic nephropathy. *Diabetes.* 2006;55(11):2993–3003. doi:10.2337/db06-0477
43. Umanath K, Lewis JB. Update on Diabetic Nephropathy: core Curriculum 2018. *Am J Kidney Dis.* 2018;71(6):884–895. doi:10.1053/j.ajkd.2017.10.026
44. Khan TA, Kalsoom K, Iqbal A, et al. A novel missense mutation in the NADPH binding domain of CYBB abolishes the NADPH oxidase activity in a male patient with increased susceptibility to infections. *Microb Pathogenesis.* 2016;100:163–169. doi:10.1016/j.micpath.2016.09.020
45. Wang J, Wang L, Pang Z, et al. Integrated Analysis of Ferroptosis and Immunity-Related Genes Associated with Diabetic Kidney Disease. *Diabetes Metab Syndr Obes Targets Ther.* 2023;16:3773–3793. doi:10.2147/DMSO.S434970
46. Jialal I, Jialal G, Adams-Huet B, et al. Neutrophil and monocyte ratios to high-density lipoprotein-cholesterol and adiponectin as biomarkers of nascent metabolic syndrome. *Hormone Mol Biol Clin Invest.* 2020;41(2). doi:10.1515/hmbci-2019-0070
47. Chen T, Tu M, Huang L, et al. Association of Serum Adiponectin with Intima Media Thickness of Dorsalis Pedis Artery and Macroangiopathy in Type 2 Diabetes. *J Diab Res.* 2020;2020(4739271):1–10. doi:10.1155/2020/4739271
48. Devarajan P. Emerging biomarkers of acute kidney injury. *Contrib Nephrol.* 2007;156:203–212. doi:10.1159/000102085
49. Nielsen SE, Schjoedt KJ, Astrup AS, et al. Neutrophil Gelatinase-Associated Lipocalin (NGAL) and Kidney Injury Molecule 1 (KIM1) in patients with diabetic nephropathy: a cross-sectional study and the effects of lisinopril. *Diabetic Med.* 2010;27(10):1144–1150. doi:10.1111/j.1464-5491.2010.03083.x
50. Zachwieja J, Soltysiak J, Fichna P, et al. Normal-range albuminuria does not exclude nephropathy in diabetic children. *Pediatr Nephrol.* 2010;25(8):1445–1451. doi:10.1007/s00467-010-1443-z
51. Lacquaniti A, Donato V, Pintaudi B, et al. "Normoalbuminuric" diabetic nephropathy: tubular damage and NGAL. *Acta diabetologica.* 2013;50(6):935–942. doi:10.1007/s00592-013-0485-7



Journal of Inflammation Research

Dovepress

### Publish your work in this journal

The Journal of Inflammation Research is an international, peer-reviewed open-access journal that welcomes laboratory and clinical findings on the molecular basis, cell biology and pharmacology of inflammation including original research, reviews, symposium reports, hypothesis formation and commentaries on: acute/chronic inflammation; mediators of inflammation; cellular processes; molecular mechanisms; pharmacology and novel anti-inflammatory drugs; clinical conditions involving inflammation. The manuscript management system is completely online and includes a very quick and fair peer-review system. Visit <http://www.dovepress.com/testimonials.php> to read real quotes from published authors.

Submit your manuscript here: <https://www.dovepress.com/journal-of-inflammation-research-journal>